

Potential impact of CV-QKD integration on classical WDM network capacity

Cédric Ware, *Senior Member, IEEE*, Raphaël Aymeric, Chaïma Zidi, Mounia Lourdiāne

Abstract—Continuous-variable quantum key distribution (CV-QKD) could allow QKD and classical optical signals physically sharing the same optical fibers in existing networks. However, Raman scattering imposes a limit on the optical power, which in turn impacts the network capacity for classical traffic in presence of CV-QKD. Network-planning simulations indicate that maxing out the CV-QKD capacity in an optical link can adversely impact its classical capacity. Although preliminary, these results show that designing a mixed classical and CV-QKD network will require dedicated planning heuristics and tools that specifically seek a compromise between classical and CV-QKD traffics.

Index Terms—Optical Networking, Network Capacity, Quantum Key Distribution, CV-QKD.

I. INTRODUCTION

QUANTUM-KEY DISTRIBUTION (QKD) is often presented as a future-proof physical-security solution to the key distribution problem. Within that field, continuous-variable (CV) QKD uses the same type of coherent-detection optical receivers as classical data traffic, which gives it the potential not only to share hardware with classical channels, but also—and of great interest to network operators—to physically coexist with them in the same optical fibers through wavelength-division multiplexing (WDM), using the intrinsic spectral-filtering property of coherent detection [1], [2]. We recently demonstrated experimentally a symbiotic operation of CV-QKD and classical communication where the latter is actually used as a reference signal for phase and frequency recovery on the quantum channel [3]. The big drawback of CV-QKD compared to alternatives is its shorter range: beyond a certain propagation length, due to attenuation in the fiber, the key rate drops sharply; In [4] the theoretical key rate is calculated depending on a number of parameters, including attenuation, but also various noise-generating processes. Among those, Raman scattering results in a crosstalk-like noise between WDM channels, a significant limiting factor if CV-QKD is to coexist with classical traffic. The aforementioned references [1]–[4] study CV-QKD key rate, including in the case of coexistence with intense WDM channels, but for a single optical link, not in a complete network. On the other hand, quantum network capacity and design tools have been studied [5], but without coexistence.

This paper searches a limit on the coexistence of both signals within a network. Since CV-QKD is impeded by

Cédric Ware and Raphaël Aymeric are with LTCI, Télécom Paris, Institut Polytechnique de Paris, Palaiseau, France. Mounia Lourdiāne is with SAMOVAR, Télécom SudParis, Institut Polytechnique de Paris, Évry, France. Chaïma Zidi was formerly with both institutions mentioned above.

© 2022 IEEE. Personal use of this material is permitted. Permission from IEEE must be obtained for all other uses, in any current or future media, including reprinting/republishing this material for advertising or promotional purposes, creating new collective works, for resale or redistribution to servers or lists, or reuse of any copyrighted component of this work in other works.

TABLE I
PHYSICAL, TECHNOLOGICAL AND SIMULATION PARAMETERS.

Maximum classical WDM channels per fiber	N	40
Classical data rate per WDM channel	\mathcal{R}	100 Gbit/s
Classical optical power per WDM channel	P_{opt}	0 dBm
Optical fiber attenuation	α_L	0.2 dB/km
Insertion loss on quantum channel	α_0	2 dB
CV-QKD symbol rate	f_{sym}	1 Gbaud
CV-QKD reconciliation efficiency	β	0.95
CV-QKD detection type	μ	2 (heterodyne)
CV-QKD receiver fixed noise	ξ_0	10^{-3} SNU
CV-QKD Raman noise efficiency	ξ_R	variable, SNU/W
Maximum paths per node pair in RWA	k	5
Distance scaling factor	Λ	0.01–0.2

the optical power of classical WDM channels circulating alongside, conversely, enabling a certain amount of CV-QKD traffic in a fiber requires setting a limit on optical power, thus capping the number of WDM channels available in a given fiber for classical traffic, which in turn impacts the overall network capacity. Our simulations indicate that unless precautions are taken, above a certain threshold of CV-QKD offered traffic, optical links become unable to sustain classical traffic, effectively dropping out of the network. This sharply increases the blocking probability on the classical traffic, defined as the ratio of traffic blocked (that the network fails to carry) over the total traffic requested.

Our methodology and choice of parameter values are described in Sec. II, yielding the simulation results shown in Sec. III. We then discuss our interpretation, limits of these preliminary results, and especially ways to further investigate this problem in Sec. IV, before concluding the paper.

II. METHODOLOGY AND PARAMETERS

A. CV-QKD and classical signal parameters

We chose some “reasonable” values, summarized in table I, for a classical WDM network simulation, as well as physical and technological parameters required to calculate the CV-QKD key rate (considered in the asymptotic regime of an infinite number of quantum state exchanges). We assume that each optical link can carry CV-QKD traffic in a dedicated spectral window separate from classical WDM channels, with a secure-key rate of $K = f_{\text{sym}} \cdot r$ [4, Eq. (2.1)], where f_{sym} is the quantum channel’s symbol rate and r the secret fraction (bits per symbol transmitted), whose optimal value can be calculated numerically as a function of channel transmittivity T , excess noise ξ (defined here at channel output), efficiency of information reconciliation β and detection type μ [4, Sec. 10],

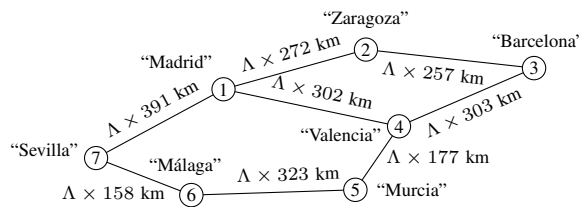


Fig. 1. Network topology with 7 nodes and 8 bidirectional (16 unidirectional) links. Distances are uniformly scaled by factor Λ .

with a 100%-efficient receiver. For a link of length L with n WDM classical signals, we assume:

$$T = 10^{-\alpha_{\text{dB}}/10} \quad (1a)$$

$$\alpha_{\text{dB}} = \alpha_0 + \alpha_L \cdot L \quad (1b)$$

$$\xi = \xi_0 + \xi_R \cdot n \cdot P_{\text{opt}} \quad (1c)$$

with α_0 a fixed insertion loss and α_L the fiber's attenuation. We use a simple linear model for ξ as a function of the per-WDM-channel optical power P_{opt} , with $\xi_0 = 10^{-3}$ shot-noise units (SNU) corresponding to the detection noise (untrusted), a value optimistically chosen, as is $f_{\text{sym}} = 1$ Gbaud. (In [3], we managed $f_{\text{sym}} = 250$ Mbaud and $\xi_0 \simeq 9 \cdot 10^{-2}$.) One major uncertainty is the choice of the Raman efficiency ξ_R , which will be specifically investigated in Sec. III-C.

B. Network simulation, topology and traffic matrix

We conducted simulations using the open-source network planning tool Net2Plan [6], in the offline network design mode, using an algorithm described below. We started from an example topology and traffic matrix representing a “Fictitious mesh network connecting the seven most populated cities in Spain”, (Fig. 1), with 7 nodes and 16 unidirectional links, and 42 traffic demands. A traffic demand is a request to carry a given amount of traffic (its “offered traffic”) between specified origin and destination node pairs. The 42 demands in this example offer between 6.95 and 1815 Gbit/s, for a total offered traffic (summed over all demands) of 10 Tbit/s. The links average 273 km each; however, since CV-QKD is usually limited to ranges up to tens of km, we rescaled all the links by a uniform factor Λ , using values between 0.01 and 0.25. For instance, with $\Lambda = 0.01$ (which could represent a campus-scale network), the longest link (1-7) is 3.9 km long and can sustain 345 Mbit/s of CV-QKD traffic; this value drops to 88 Mbit/s with $\Lambda = 0.05$ (19.6 km, e.g. city-scale); and 0 with $\Lambda = 0.1$ (39.1 km), but traffic can still be relayed through other paths. Similarly, we kept the same traffic matrix for the classical and CV-QKD traffics, uniformly scaling the total offered traffic to vary the load. For each value of the parameters, and of the classical and CV-QKD offered traffic, quantum and classical channels are allocated as described in the following sections. The CV-QKD is allocated first, getting priority over the classical traffic, as we aim to study the impact of a given QKD traffic on the classical capacity.

C. CV-QKD traffic routing heuristic: opaque

CV-QKD demands are routed as in an opaque network: given that CV-QKD is range-limited, we do not attempt any

optical bypass, which would lengthen the paths and reduce capacity. Instead, we assume each node is a trusted relay, which also aggregates the traffic from all CV-QKD demands that need the same link. Each link's CV-QKD capacity in terms of maximum key rate is calculated in the absence of Raman noise (because there is no classical traffic yet). Then, at each step, the demand with the largest amount of yet-unallocated traffic is served: the k shortest possible paths are examined, selecting the one with the largest remaining capacity, and a route is added carrying as much of the demand's traffic as possible without increasing the aggregated amount on any link beyond that link's capacity. This step is then repeated until all CV-QKD demands are served or no more routes can be added. Optionally, in some of our simulations, we kept the total CV-QKD traffic in each link below the link's capacity by a small (e.g. 1 %) margin; we will see that it has a strong impact.

D. Classical traffic RWA heuristic: transparent fixed-grid

A routing and wavelength assignment (RWA) heuristic is used to route the classical traffic demands as in a transparent network: lightpaths are created directly from origin to destination node, occupying the same WDM channel over all the links in the path (wavelength continuity), assuming each node is a perfectly flexible reconfigurable optical add-drop multiplexer (ROADM). Given the short ranges, all paths are considered classically feasible and regeneration is not considered. Each lightpath occupies 1 WDM slot and carries a fixed traffic \mathcal{R} . No provision is made to ensure that the multiple lightpaths required to serve large demands follow the same route or occupy contiguous WDM slots.

As above, demands are served in decreasing order of yet-unallocated traffic. At each step, the k shortest possible paths are examined, checking that: a WDM slot is available over the whole path; and that adding a slot to all links of the path would not reduce any link's CV-QKD capacity below the amount of CV-QKD traffic it carries. A lightpath carrying 100 Gbit/s is created over the shortest path that matches both conditions. This step is repeated until all classical demands are satisfied or no more lightpaths can be added.

III. SIMULATION RESULTS

A. CV-QKD capacity vs network scale

Figure 2(a) shows the proportion of total requested CV-QKD traffic that cannot be served without exceeding capacity on one of the links (thus “blocked”), as a function of the total offered CV-QKD traffic. In our methodology, this does not depend on the classical traffic or the Raman effect, since CV-QKD is served first. It does depend on the distance scaling factor Λ , as links' capacities change with propagation length. The network capacity, in terms of total CV-QKD traffic that can be carried with negligible blocking, is about 0.7–2 Gbit/s for $\Lambda = 0.01$ –0.05 (which brings the average link length to a few km, as in a small-to-large city network), then drops to 100–200 Mbit/s for $\Lambda = 0.1$, above which the distances become too large for any significant traffic to be carried.

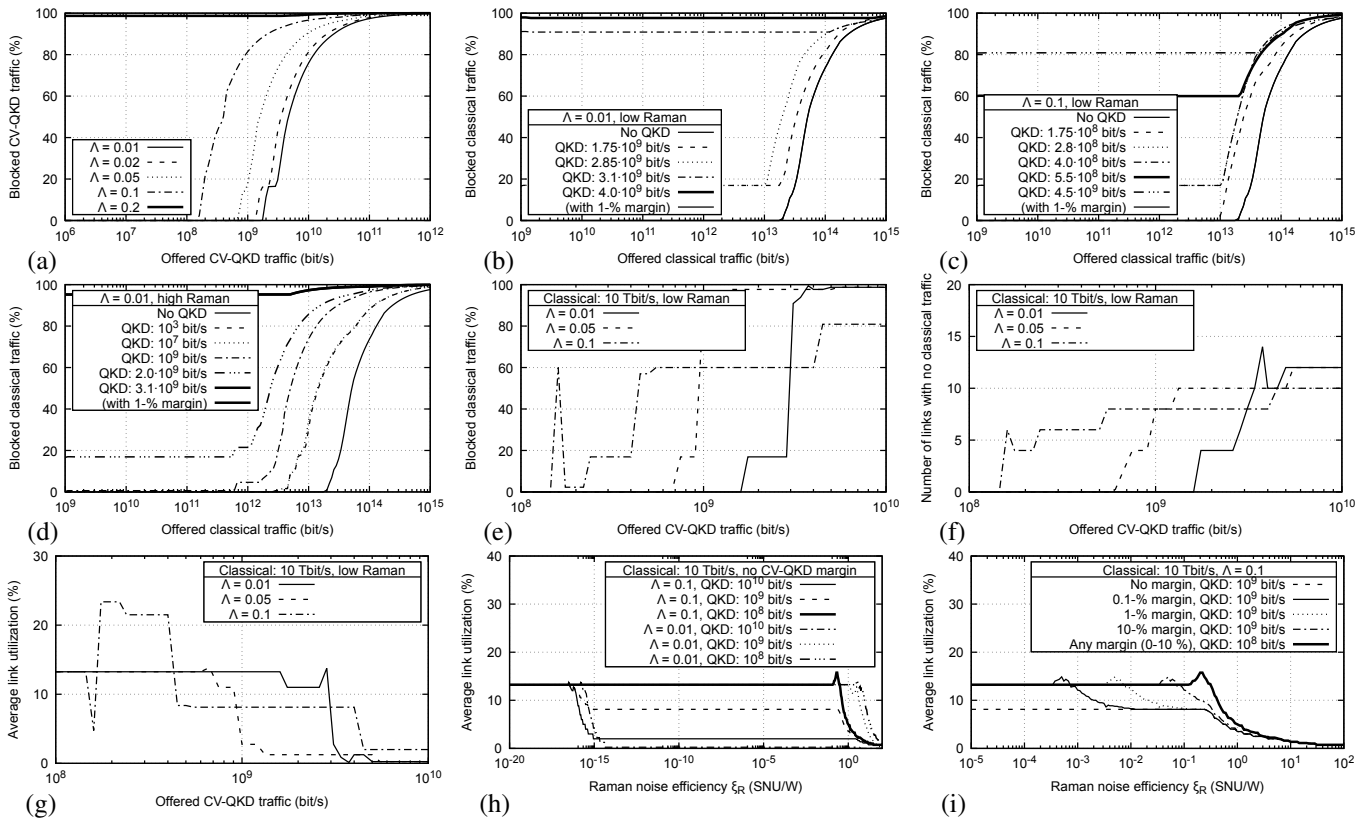


Fig. 2. (a)–(e): proportion of traffic blocked (classical or CV-QKD) as a function of network load, represented by the total offered traffic (classical or CV-QKD). Multiple values of the distance scaling factor Λ are tested; also two values of the Raman noise efficiency: $\xi_R = 10^{-12}$ SNU/W (“low Raman”) or 10 SNU/W (“high Raman”). Some plots are repeated with a 1%-margin in CV-QKD capacity, curves overlap with the no-margin curves as indicated by the line style. (f)–(g): number of links unused by classical traffic, and average link utilization (WDM slots active in the optical fibers), as a function of the offered CV-QKD traffic. (h)–(i): average link utilization as a function of ξ_R , without margin in CV-QKD capacity, and with a 0 to 10%-margin.

B. Classical capacity vs CV-QKD

Figure 2(b), (c) and (d) show the blocked classical traffic as a function of the total offered classical traffic, for several values of the offered CV-QKD traffic, using $\Lambda = 0.01$ or 0.1 , and two values for ξ_R that will be shown in Sec. III-C to be representative: 10^{-12} SNU/W (“low Raman”) and 10 SNU/W (“high Raman”). No margin is applied on the CV-QKD capacity, allowing links to carry their maximum CV-QKD traffic. The thin solid-line curve gives the classical network capacity without any CV-QKD, about 20 Tbit/s, independent of Λ due to our methodology. With CV-QKD traffic, below the values shown, in the low-Raman case, the curve is identical to the no-QKD case. Above a certain amount of CV-QKD traffic, however, a “floor” of blocking appears even for very low amounts of classical traffics. The floor increases sharply and discretely with CV-QKD traffic: note that some curves overlap for different amounts of CV-QKD traffic. This can also be seen on Fig. 2(d) for the high-Raman case, except that even with a CV-QKD traffic as low as 1 kbit/s, the classical capacity is reduced to about 3 Tbit/s.

This discrete behavior also appears on Fig. 2(e): the blocking of classical traffic increases by steps with the CV-QKD offered traffic, with even the spurious “spike” observed at $1.6 \cdot 10^8$ bit/s for $\Lambda = 0.1$ reaching the same level as a later plateau. On such a small network topology, this seems

consistent with individual links “dropping out” of the network, that is, becoming unavailable to classical traffic. This is supported by Fig. 2(f): as CV-QKD traffic increases, a number of links stop carrying classical traffic. Also, Fig. 2(g) shows the average link utilization (percentage of WDM slots in the fiber that are actually used). It starts at 13 %, comparable to the ratio of offered classical traffic (10 Tbit/s) to theoretical maximum capacity ($N\mathcal{R} \times$ number of links = 64 Tbit/s), which is 16 %; then it may increase, as classical traffic is diverted to more circuitous routes; but eventually it drops as more links become unavailable and classical demands just can't be met.

The range of CV-QKD traffic where the impact varies most (10^8 – 10^{10} bit/s) corresponds to where the CV-QKD blocking rate increases, as per Fig. 2(a). This suggests that the reason why links become unavailable to classical traffic is that CV-QKD traffic requires their maximum capacity—at which point adding any optical power to support classical traffic, even with a low Raman noise generation, reduces the capacity below the required level, which is forbidden in our methodology.

This suggests that limiting the CV-QKD traffic below the maximum by a certain margin might “unclog” the links. We redid some of the simulations corresponding to Figs. 2(b)–(d) with a 1%-margin on the links’ CV-QKD capacity. The graphs (partially shown here) are identical to Fig. 2(d) in the high-Raman case, the margin has no effect; but in the low-Raman case all the curves overlap the no-QKD curve, that is,

the impact of CV-QKD on classical traffic disappears entirely.

C. Choice of Raman noise efficiency

In our model, the Raman noise efficiency ξ_R is a simplistic assessment of Raman nonlinear scattering. We will attempt to show empirically that a more realistic model isn't actually necessary at this stage of the investigation.

As a starting point, the experimental value from [1, Fig. 5] is about 11 SNU/W for a 25-km propagation length. Other references exhibit similar, sometimes lower values. Experimental conditions vary, especially the isolation (spectrally or otherwise) between the quantum and classical signals. As conditions may improve, we also want to test lower ξ_R values.

Figure 2(h) shows the average link utilization for a classical traffic of 10 Tbit/s, as a function of ξ_R , from 10^{-20} to 10^2 SNU/W. Three different regimes appear: at very low ξ_R ($\leq 10^{-16}$ SNU/W), link utilization remains high; then a long plateau (10^{-15} – 10^{-1}) where the impact of CV-QKD on classical traffic remains constant; and finally the impacts worsens at higher values. The first regime could be a numerical artifact: at such low values, floating-point numbers might not have enough precision to show the drop in CV-QKD key rate due to the Raman noise. Given the unlikelihood that Raman noise is so low anyway, we ignored this regime, and chose to perform the other simulations with values representative of the other two: $\xi_R = 10^{-12}$ SNU/W (“low Raman”, on the plateau) and $\xi_R = 10$ SNU/W (“high Raman”, in the worsening regime). This seemed sufficient in the no-margin case. Several simulations were checked with $\xi_R = 10^{-3}$ SNU/W, and yielded exactly the same results as with 10^{-12} .

On the other hand, Fig. 2(i) shows the same graph but with several values of the margin on the CV-QKD capacity. Here link utilization remains at its high starting level up to a ξ_R that depends on the margin and possibly the CV-QKD traffic, then starts dropping as before. This suggests that in some cases (though not e.g. with the lowest CV-QKD traffic), a margin helps maintain classical capacity if Raman efficiency is low.

IV. DISCUSSION AND QUESTIONS FOR FUTURE WORK

The results above indicate that CV-QKD traffic significantly impacts classical network capacity in some cases, especially if Raman noise turns out to be high. However, this study is still preliminary, opening several potential lines of investigation.

The specificity of the network topology and traffic matrix: we only studied one small topology where discrete effects can be seen when optical links become unavailable for classical traffic. It would be interesting to identify which links are affected first; at a guess, the longest links should be more vulnerable. Also, in a more complex topology, especially one more densely-meshed, would the higher number of alternate paths between nodes compensate the drop in capacity?

Keeping a CV-QKD capacity margin or using smarter heuristics: limiting the CV-QKD traffic in each link slightly below the maximum capacity seems to help, but how much margin is needed remains to be investigated. Given that it depends on the Raman efficiency, this may require a more realistic model as well. Alternatively, more advanced planning

heuristics and design tools could find better compromises between classical and CV-QKD traffic, e.g. with priority management between the CV-QKD and classical traffic matrices.

What is the actual Raman noise, if needed: our linear model may be sufficient to show that an impact exists, but it does not accurately represent the physical reality of Raman noise generation. The question is open of how much accuracy is actually needed: the value of the required CV-QKD capacity margin certainly depends on the Raman noise, but is this dependence very sensitive, or could a rough estimate be satisfactory? The answer will certainly also depend on the spectral distance between the CV-QKD signal and the classical WDM channels—which may in turn determine whether CV-QKD can be carried in wavelengths close to standard WDM bands or a completely separate spectral band must be allotted.

V. CONCLUSION

We have shown in network-planning simulations that coexistence of CV-QKD and classical traffic in the same optical fibers can in some cases have an adverse impact on the classical network capacity, due to the need to preserve CV-QKD traffic from excessive Raman noise. Precautions can be taken, such as limiting the amount of CV-QKD traffic slightly below each optical link's maximum capacity, but how much margin is required remains an open question. We have pointed out this and other potential lines of investigation. In any case, it seems that designing a mixed classical and CV-QKD network will require dedicated planning heuristics and tools.

ACKNOWLEDGMENTS

This project has received funding from the European Union's Horizon 2020 research and innovation programme under grant agreement No 820466 (Quantum-Flagship project CiViQ: Continuous-Variable Quantum Communications). Also, this research was partially supported by Labex DigiCosme (project ANR-11-LABEX-0045-DIGICOSME), operated by ANR as part of the program “Investissement d'Avenir” Idex Paris-Saclay (ANR-11-IDEX-0003-02).

REFERENCES

- [1] R. Kumar, H. Qin, and R. Alléaume, “Coexistence of continuous variable QKD with intense DWDM classical channels,” *New Journal of Physics* **17** no. 4, (2015) 043027, [arXiv:1412.1403](https://arxiv.org/abs/1412.1403) [quant-ph].
- [2] T. A. Eriksson, T. Hirano, B. J. Putnam, G. Rademacher, R. S. Luis, M. Fujiwara, R. Namiki, Y. Awaji, M. Takeoka, N. Wada, *et al.*, “Wavelength division multiplexing of continuous variable quantum key distribution and 18.3 Tbit/s data channels,” *Communications Physics* **2** no. 9, (2019) 1–8.
- [3] R. Aymeric, Y. Jaouën, C. Ware, and R. Alléaume, “Symbiotic joint operation of quantum and classical coherent communications,” in *Optical Fiber Communication Conference*, no. W2A.37. Mar., 2022. [arXiv:2202.06942](https://arxiv.org/abs/2202.06942) [quant-ph]. Poster.
- [4] F. Laudenbach, C. Pacher, C.-H. F. Fung, A. Poppe, M. Peev, B. Schrenk, M. Hentschel, P. Walther, and H. Hübner, “Continuous-variable quantum key distribution with gaussian modulation—the theory of practical implementations,” *Advanced Quantum Technologies* (2018) 1800011, [arXiv:1703.09278](https://arxiv.org/abs/1703.09278) [quant-ph].
- [5] K. Azuma, S. Bäuml, T. Coopmans, D. Elkouss, and B. Li, “Tools for quantum network design,” *AVS Quantum Science* **3** no. 1, (2021) 014101, [arXiv:2012.06764](https://arxiv.org/abs/2012.06764) [quant-ph].
- [6] P. Pavon-Marino and J.-L. Izquierdo-Zaragoza, “Net2plan: an open source network planning tool for bridging the gap between academia and industry,” *IEEE Netw.* **29** no. 5, (2015) 90–96.